applied sciences

MDPI

Article

Cow Dung Ash in Mortar: An Experimental Study

Muluken Alebachew Worku [1], Woubishet Zewdu Taffese [2,3,*], Behailu Zerihun Hailemariam [3] and Mitiku Damtie Yehualaw [3,*]

[1] Department of Construction Technology and Management, Woldia Institute of Technology, Woldia University, Woldia 7220, Ethiopia
[2] School of Research and Graduate Studies, Arcada University of Applied Sciences, Jan-Magnus Jansson Aukio 1, 00560 Helsinki, Finland
[3] Faculty of Civil and Water Resource Engineering, Bahir Dar Institute of Technology, Bahir Dar University, Bahir Dar 6000, Ethiopia
* Correspondence: woubishet.taffese@arcada.fi (W.Z.T.); mtkdmt2007@gmail.com (M.D.Y.)

Abstract: This study investigated the impact of using cow dung ash (CDA) as a partial replacement for ordinary Portland cement (OPC) in mortar. Mortar mixes are prepared by replacing OPC with CDA at varying levels: 5%, 10%, 15%, 20%, 25%, and 30%. The chemical composition of CDA shows that it is composed primarily of SiO_2, Al_2O_3, and Fe_2O_3, with a significant amount of loss of ignition. The workability, hardened properties, and microstructure of CDA-containing mortars are also analyzed. The increasing CDA content in mortar reduces workability and, beyond 5%, it causes high water absorption due to CDA's porous nature and unremoved organic compounds. This impacts the density and compressive strength of the hardened mortar as well as compromising its homogeneous characteristics. When using 5% CDA, the bulk density and compressive strength of the mortar are comparable to those of the control mixes. Nonetheless, as the proportion of CDA increases, both the bulk density and compressive strength of the mortar diminish. The thermal stability of mortar mixes with 10%, 20%, and 30% CDA is unaffected at temperatures between 500 °C and 600 °C. The Fourier-transform infrared spectroscopy (FTIR) analysis reveals the presence of unreacted particles and wide stretched C–S–H gels in the mortar samples. In general, the results suggest that CDA can be utilized as a substitute for OPC at a ratio of up to 10% in the manufacturing of mortar and can serve as a feasible alternative cementitious material.

Keywords: cow dung ash; mortar; microstructure; workability; durability; sustainability; supplementary cementitious materials; carbon footprint

check for updates

Citation: Worku, M.A.; Taffese, W.Z.; Hailemariam, B.Z.; Yehualaw, M.D. Cow Dung Ash in Mortar: An Experimental Study. *Appl. Sci.* **2023**, *13*, 6218. https://doi.org/10.3390/app13106218

Academic Editors: Francisco B. Varona Moya and Mariella Diaferio

Received: 17 April 2023
Revised: 15 May 2023
Accepted: 15 May 2023
Published: 19 May 2023

Copyright: © 2023 by the authors. Licensee MDPI, Basel, Switzerland. This article is an open access article distributed under the terms and conditions of the Creative Commons Attribution (CC BY) license (https://creativecommons.org/licenses/by/4.0/).

1. Introduction

The construction sector is a vital and rapidly expanding industry worldwide, playing a crucial part in the economic growth and development of nations. As construction projects continue to grow across numerous developing nations, there will be a consistent rise in the need for concrete, since no other material compares to it in terms of strength and accessibility. However, the concrete industry is one of the largest consumers of natural resources and contributes significantly to global anthropogenic carbon dioxide (CO_2) emissions. According to the Global Cement and Concrete Association (GCCA), 14 billion cubic meters of concrete are produced every year for use in the construction of roads, bridges, tunnels, houses, dams, and flood defenses [1]. The primary source of high CO_2 levels in the concrete industry is the production of Portland cement, which is the main binder and accounts for approximately 8% of global CO_2 emissions with an annual production of more than four billion tons [2,3]. Taking this into account, cement and concrete manufacturers are working to accelerate the transition to greener concrete by committing to reducing CO_2 emissions by 25% by 2030 and meeting a target aligned with the Paris Agreement to limit global warming to 1.5 °C [1].

Reducing carbon emissions from the cement industry is a significant challenge, but there are several approaches that can be taken. One of the most practical, economical, and sustainable approaches to reducing the CO_2 emissions caused by the concrete industry is the use of a sustainable system loop that can transform waste resources into valuable products. This approach provides a range of advantages that go beyond reducing clinker content and associated carbon emissions. It enables a reduction in the use of conventional cement ingredients such as limestone, thereby conserving valuable natural resources. Moreover, repurposing waste materials that would otherwise end up in landfills promotes waste reduction and diversion, thereby fostering more sustainable waste management practices.

In the past two decades, several studies have already explored supplementary cementitious materials (SCMs) derived from industrial and agricultural byproducts [4–11]. These include silica fume, fly ash, blast furnace slag, rice husk ash, coffee husk ash, ground nut ash, bamboo leaves ash, banana leaves ash, sugarcane bagasse ash, corncob ash, animal bone ash, tobacco waste ash, glass powders, coal bottom ash, and eggshell ash. Several studies have also investigated the potential of waste materials to replace various ingredients used in concrete production, including the use of recycled aggregates, coconut fibers, glass, marble, and rubber tree seeds [12–18]. The objective is to conserve natural resources and address the environmental impact caused by these waste materials. By substituting conventional ingredients for waste materials, the concrete industry can contribute to resource conservation and mitigate the burden on the environment.

In recent years, researchers have studied the potential of cow dung ash (CDA) as a supplementary cementitious material. Cow dung, a byproduct of cattle farming, is known for being a rich source of silicon dioxide, and thus has pozzolanic properties [19]. It also contains organic matter, including fibrous materials that have passed through the cow's digestive system. The chemical composition of cow dung typically consists of carbon, nitrogen, hydrogen, oxygen, and phosphorus, as well as potassium and calcium [20]. Ekasila et al. [21] investigated the effectiveness of using 10% CDA and 20% rice husk ash (RHA) in concrete under varying curing conditions. The researchers concluded that incorporating both SCMs in the concrete resulted in greater strength. Another study was conducted to evaluate the performance of concrete with 15% CDA that was exposed to water [22]. The specimens were cured for 28 days and then exposed to fresh water for different durations of time: 56, 90, 180, and 365 days. The results showed that the concrete with CDA had superior pH, compressive and split tensile strength, and durability compared to normal concrete. The researchers also observed a lower bacterial density in the CDA-containing concrete.

According to Statista, Ethiopia has a significant population of cattle, ranking fifth in the world and holding the top spot in Africa for total count. The primary use of cow dung in Ethiopia is as a source of fertilizer, and it is also dried to serve as fuel for cooking purposes. With the Ethiopian government's ambitious plan to provide electricity to all citizens by 2025 [23], the rural population of the country will eventually shift towards using electricity for energy, potentially resulting in wasted cow dung. Therefore, it is necessary to explore alternative plans for utilizing this free and valuable resource. Considering that cement is extensively used in building construction in Ethiopia and is responsible for the highest embodied energy and CO_2 emissions [24], incorporating cow dung ash as a supplementary cementitious material presents a promising solution for addressing the environmental challenges stemming from both the cement industry and cow dung waste.

This paper aims to investigate the viability of using CDA as a partial replacement for ordinary Portland cement (OPC) in mortar production. This study stands out from other research on the topic by conducting a thorough investigation of the impact of CDA on various properties of mortar when used as a partial replacement for OPC. Unlike previous studies that focused on a limited set of factors, this work evaluated a range of parameters, including workability, water absorption, bulk density, compressive strength, homogeneity, surface attack resistance, thermal decomposition, and mineralogical composition. Additionally, as the properties of cow dung can be affected by multiple factors, the findings of

this study are significant and novel, as no prior research has been carried out on this topic in the particular region where the study was conducted.

2. Materials and Methods

2.1. Materials

2.1.1. Cement

The OPC used in this study had a 42.5R grade and was sourced from Dangote Cement Plc. The quality of the cement was assessed as per ASTM C1084 [25]. The grading and physical properties were in conformity with the requirements necessitated by standard specifications of ASTM C150/C150M [26].

2.1.2. Fine Aggregate

Fine aggregate was obtained from impurity-free river sand in Lalibela, Ethiopia. The sand was subjected to various tests to ensure its quality met the ASTM standard. Figure 1 shows the fine aggregate gradation curve result of the sieve analysis test as per the standard ASTM C117 [27]. In addition to this, other physical property evaluations were conducted on the sand samples, and the undertaken test results are outlined in Table 1, with reference to their respective test standards.

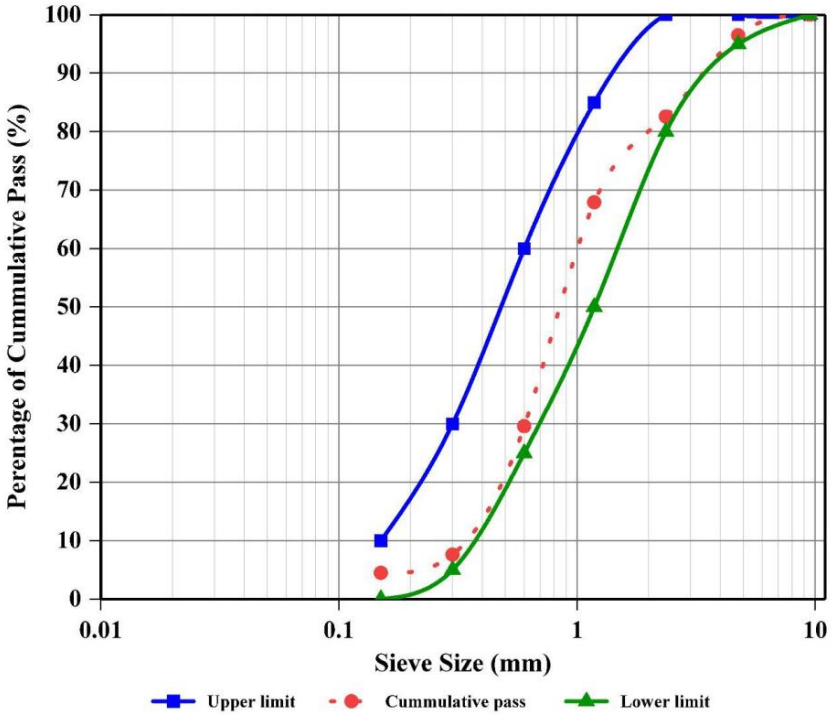

Figure 1. Fine aggregate gradation curve.

Table 1. Test results of the fine aggregate.

No.	Test Type	Test Standards	Test Result	Unit
1	Fineness modulus	ASTM C117	3.11	[-]
2	Loose bulk density	ASTM C29/C29M	1779.63	[Kg/m^3]
3	Compacted bulk density	ASTM C29/C29M	1885.46	[Kg/m^3]
4	Voids	ASTM C29/C29M	35.60	[%]
5	Specific gravity	ASTM C128	2.70	[-]
6	Water absorption	ASTM C128	3.36	[%]
7	Free moisture content	ASTM C566	2.50	[%]
8	Silt content	ASTM C136	3.50	[%]

2.1.3. Cow Dung Ash

The cow dung samples were obtained from the cattle production area surrounding the city of Bahir Dar, Ethiopia. The samples were sun-dried for a week and subsequently calcined in a muffle furnace at 800 °C for 2 h. This particular temperature was chosen as it was found to yield CDA of superior quality [28]. Once burned, the samples were allowed to cool and then ground using a milling machine. Samples that passed through a sieve size of 150 µm were used for cement replacement. The resulting cow dung ash had a dark gray appearance, as shown in Figure 2.

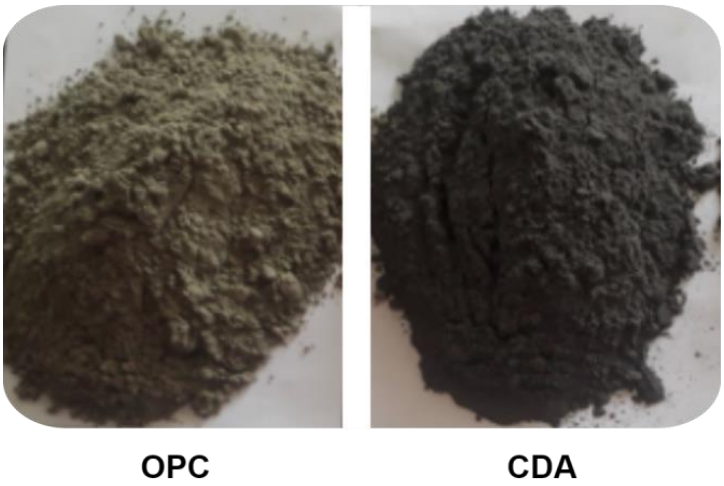

Figure 2. A visual representation depicting the OPC and CDA utilized in the study.

Table 2 compares the results of the X-ray fluorescence (XRF) test conducted on the CDA with the chemical requirements specified by ASTM C150/C150M for Portland cement. The test results indicated that the CDA contained 16.66% SiO_2, 6.15% Al_2O_3, and 7.4% Fe_2O_3, with a negligible amount of SO_3. The sum of the silicious oxides was 30.21%, which did not meet the minimum requirements specified by the standard. The content of MgO, a chemical component found in CDA, falls within the range specified by ASTM C150/C150M for OPC. The loss of ignition (LOI) in the CDA was found to be over 34%, whereas the maximum limit specified by the ASTM is 5% for OPC. This suggests that there are high amounts of unburned inorganic materials present in the CDA, which could result in reduced density and strength.

Table 2. CDA composition analysis and its correlation with the ASTM standard for OPC.

Chemical Compositions	Oxide Content [%]	
	CDA	OPC (ASTM C150/C150M)
CaO	8.18	61–67
SiO_2	16.66	19–23
SO_3	0	0–5.35
Al_2O_3	6.15	2.5–6
Fe_2O_3	7.4	0.1–5
MgO	4.72	1–5
LOI	34.13	-
Na_2O	4	-
K_2O	5.92	-
MnO	0.26	-
P_2O	7.59	-

2.1.4. Mortar Mix Preparation

The mortar mixes were prepared using a water-to-binder ratio of 0.51 and a volumetric ratio of 1:2.75 for cement and sand. As the main objective of our study was to explore the

effects of partially replacing OPC with CDA, we examined different levels of CDA content, ranging from 5% to 30%, in increments of 5% (i.e., 5%, 10%, 15%, 20%, 25%, and 30%). A total of 336 cubes, three samples for each mix, were produced specifically for the purpose of performing tests on the hardened mortar properties. Table 3 illustrates the mix codes and the percentages of OPC and CDA used, along with their respective quantities. The table also presents the quantity of potable tap water used to mix the mortar for each mix series.

Table 3. Proportions and quantities of materials in mortar mixtures.

Mix Code	OPC Content		CDA Content		Water	Sand
	[%]	[kg]	[%]	[kg]	[kg]	[kg]
CDA0	100	3.219	-	0	1.631	8.85
CDA5	95	3.058	5	0.161	1.631	8.85
CDA10	90	2.892	10	0.321	1.628	8.84
CDA15	85	2.725	15	0.481	1.625	8.82
CDA20	80	2.56	20	0.64	1.621	8.8
CDA25	75	2.395	25	0.798	1.618	8.78
CDA30	70	2.231	30	0.956	1.615	8.76

2.2. Methods

After conducting multiple tests on the material characteristics of cement, fine aggregates, and CDA, the workability, hardened, and microstructural properties of the control and CDA-containing mortar specimens were assessed using the test methods and types presented in Table 4. These methods adhere to ASTM standards. The properties of hardened mortar consist of water absorption, bulk density, compressive strength, homogeneity, and resistance to sulfate attack. To carry out these tests, the mortar mixes were molded into 50 mm × 50 mm × 50 mm cubes. After molding, the cubes were covered with plastic sheets and stored at room temperature for 24 h. The cubes were then removed from the molds and submerged in water for curing until the time of the test, which occurred at 3, 7, 28, 56, and 91 days. To analyze the microstructural properties of mortar specimens containing CDA, selected samples underwent thermogravimetric analysis (TGA) and Fourier-transform infrared (FTIR) spectroscopy.

Table 4. The fresh, hardened, and microstructural properties test results of the mortars.

Test Category	Properties	Test Standards	Examined Samples	Curing Ages
Fresh	Workability	ASTM C1437	All	-
Hardened	Water absorption	ASTM C1403	All	3, 7, 28 and 56 days
	Bulk density	ASTM C642		
	Compression strength	ASTM C109/C109M		
	Homogeneity	ASTM C597		
	Sulfate attack resistance	ASTM C1012		
Microstructure	Thermal decomposition	-	CDA0, CDA10, CDA30	28 days
	Mineralogical composition	-		7 and 28 days

3. Results and Discussion

This section covers the test results and discusses the impact of cow dung ash as a partial replacement for cement in the mortar specimens. Our focus is on how CDA influences the workability, hardened properties, and microstructure of the mortar specimens compared to the reference specimens that used only ordinary Portland cement.

3.1. Effects of CDA on Workability

The workability or fresh property of the plastic mortar was determined by measuring its consistency using the flow table method in accordance with ASTM C1437. The result

of this test is shown in Figure 3. As can be observed from this figure, the slump of the mortar decreased significantly with increasing levels of CDA replacement. The greatest reductions in slump were observed for CDA replacement levels of 25% and 30%, with slumps decreasing by 68% and 90%, respectively, compared to the reference mix (CDA0). Similar findings were reported by [29,30]. This phenomenon is primarily attributed to the higher porosity of CDA particles in comparison to cement. The porous nature of CDA particles leads to an increased absorption of mixing water within the mixture, especially as the proportion of CDA in the mixture increases. Consequently, compensating for the reduced workability resulting from CDA utilization necessitates a higher quantity of superplasticizer to maintain the desired workability of the mortar. According to ASTM C1437, the initial flow of the mortar should be 110 ± 5%. Hence, only the fresh mortar containing 15% CDA met this requirement.

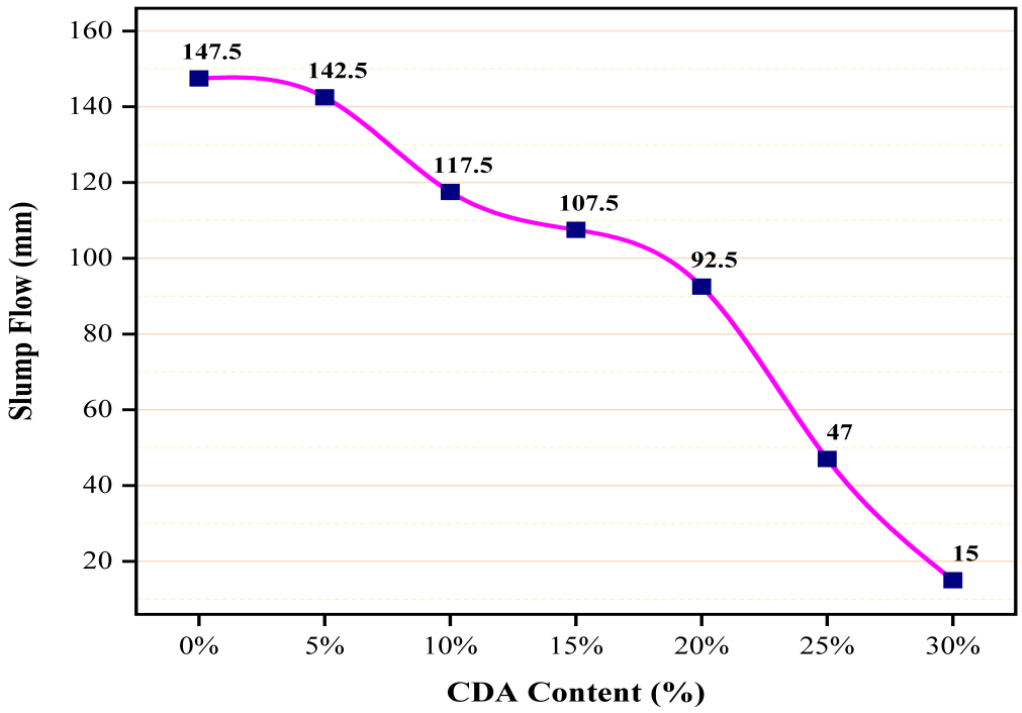

Figure 3. Slump flow of fresh mortar mixes.

3.2. Effects of CDA on Hardened Mortar Properties

3.2.1. Water Absorption

The water absorption test results are presented in Table 5, which reveal that the water absorption of the mortar specimens increased as the percentage of CDA content increased at all curing ages. The increased water absorption can be ascribed to the porous characteristics of CDA particles, as these particles possess a significant capacity to absorb water. This effect becomes particularly pronounced as the content of CDA in the mixture increases. The findings regarding water absorption align well with the observed workability of the mixture. However, it should be noted that the absorption capacity of the CDA-blended mortar decreased with longer curing periods, as reported by [31]. At a curing age of 56 days, the highest water absorption of 11.34% was observed when the CDA content was 30%, resulting in an increase of approximately 36% compared to the reference mix (8.35%). On the other hand, the lowest water absorption was 9.71% at a CDA content of 5%. The water absorption of the mortar samples with CDA content beyond 15% exceeded the maximum allowable limit of 10% [32]. It is important to note that lower water absorption is associated with lower porosity percentage and better compressive strength of the mortar paste [33].

Table 5. Water absorption of the reference and CDA-containing mortar specimens.

CDA Content	Water Absorption [%]			
	3rd Day	7th Day	28th Day	56th Day
0%	10.03	9.90	9.74	8.35
5%	10.64	10.54	10.14	9.71
10%	11.05	10.96	10.20	9.75
15%	11.38	11.25	11.12	9.78
20%	11.90	11.49	11.46	11.04
25%	12.15	11.34	11.30	11.22
30%	12.30	12.10	11.80	11.34

3.2.2. Bulk Density

The bulk density test results are presented in Table 6. From the presented table, it is evident that the bulk density of all mortar specimens incorporating CDA decreases as the percentage of CDA used as a partial replacement for cement increases. This decline in bulk density can be attributed to the utilization of CDA, which hampers the formation of dense and compacted microstructures within the mortar. This observation is supported by the results of microstructural tests discussed in Section 3.3. The bulk density of all cube specimens, including the control mixes, was found to be highest at 56 days of curing and lowest at 3 days of curing. It can be observed that the bulk density of the mortar improved as the curing ages increased from day 3 to day 56. The bulk density of the mortar blended with 5% CDA at 28 days was approximately similar to that of the control mix. Moreover, all sample cubes met the minimum bulk density requirement of 1500 kg/m^3. A similar investigation was also reported by [20].

Table 6. The bulk density of the reference and CDA-containing mortar specimens.

CDA Content	Bulk Density [Kg/m^3]			
	3rd Day	7th Day	28th Day	56th Day
0%	2568.80	2585.60	2589.86	2594.40
5%	2560.00	2582.00	2588.00	2590.40
10%	2493.34	2558.67	2561.34	2576.00
15%	2489.34	2498.00	2555.08	2560.00
20%	2466.66	2480.00	2513.20	2544.00
25%	2452.00	2464.00	2492.50	2504.00
30%	2428.00	2460.00	2480.96	2488.00

3.2.3. Compressive Strength

Figure 4 illustrates the cube compressive strength of mortar specimens at different curing periods with varying percentages of cow dung ash. It can be observed from Figure 4 that there was a linear decrease in the compressive strength of the mortar with an increase in the percentage of CDA used, and the greatest reduction was observed for the specimens containing 30% CDA across all curing periods. The observed reduction in compressive strength is expected, given that the water absorption increased and bulk density decreased with increasing CDA content. The slow rate of strength development can be attributed to the low CaO content present in CDA. As a result, the formation of the C-S-H gel is hindered due to the reduction in cement content. Additionally, the presence of pozzolanas, known for reducing early strength and slowing down hydration, contributes to this delayed strength development. Regardless, in all cases, the strength of the mortar improved as the curing period progressed. The highest compressive strength, measuring 40.79 MPa, was achieved after 56 days, while the lowest value of 15.07 MPa was recorded after 3 days of curing. Based on the findings, there was no significant difference in the compressive strength of specimens containing 5% CDA and those in the control mix, and this result is consistent with the findings reported in [30]. Moreover, even at 15% replacement of cement with CDA,

the reduction in compressive strength at the age of 56 days was not found to be significant. In comparison to the control mix sample, it was observed that at a curing time of 28 days, the compressive strength of the mortar specimens containing 20%, 25%, and 30% CDA decreased by 5.66 MPa, 6.51 MPa, and 8.87 MPa, respectively. As per the Indian Standard, IS 2250 [34], the cement and sand mortar should have a minimum compressive strength of 11.5 MPa and 17.5 MPa at the end of 3 and 7 days, respectively. It can be observed that all the mortars containing CDA samples met the specified standards.

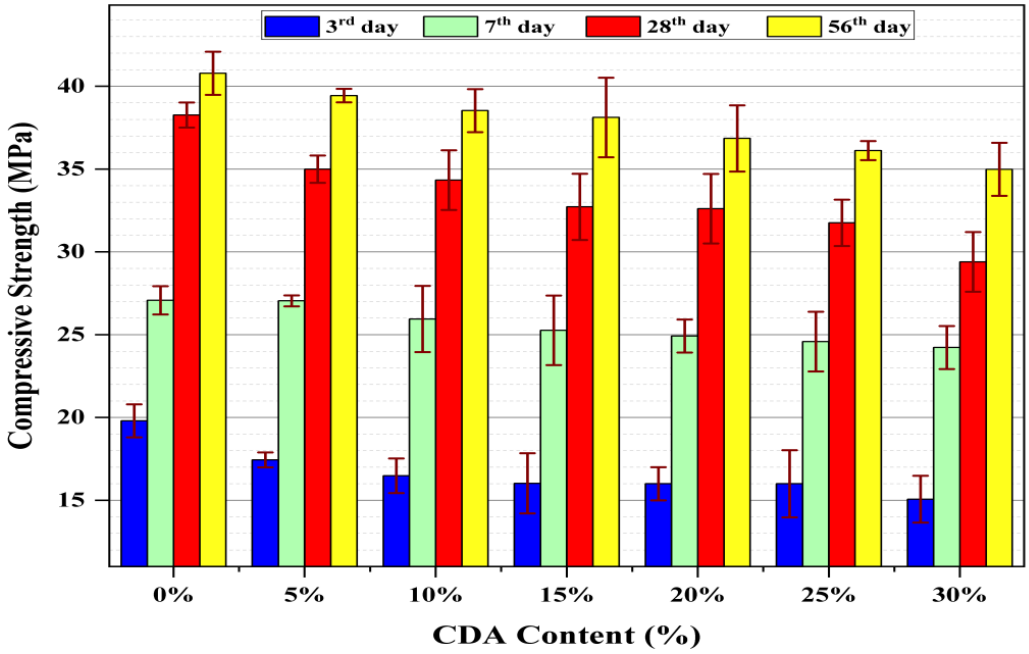

Figure 4. The compressive strength of mortar cubes.

3.2.4. Homogeneity

Figure 5 displays the results of the ultrasonic pulse velocity (UPV) test conducted to evaluate the homogeneity of the reference and CDA-containing mortar specimens. It is evident from Figure 5 that the ultrasonic pulse velocity of the mortar decreased with an increase in the percentage of CDA. The results suggest that the homogeneous characteristics of the mortar are compromised with an increase in the percentage of CDA. The trend observed in the results of the UPV test is consistent with the findings of the compressive strength tests. The experimental results indicate that the UPV values for CDA percentages of 0% to 30% were 2900–1814 m/s, 2900–954 m/s, 3100–1954 m/s, and 3280–2742 m/s after 3, 7, 28 and 56 days of curing age, respectively. As observed from the figure, there were no significant differences in the UPV values between the 3rd and 7th day results; however, the UPV values changed remarkably after later ages. The 28th day UPV results were 4.5–11.5% higher than the respective 7th day results, and the 56th day UPV results were 5–28.7% higher than the respective 28th day results. According to IS 13311 (Part 1): 1992 [35], the quality of the mortar in terms of uniformity was medium strength up to 25% CDA cement substitute.

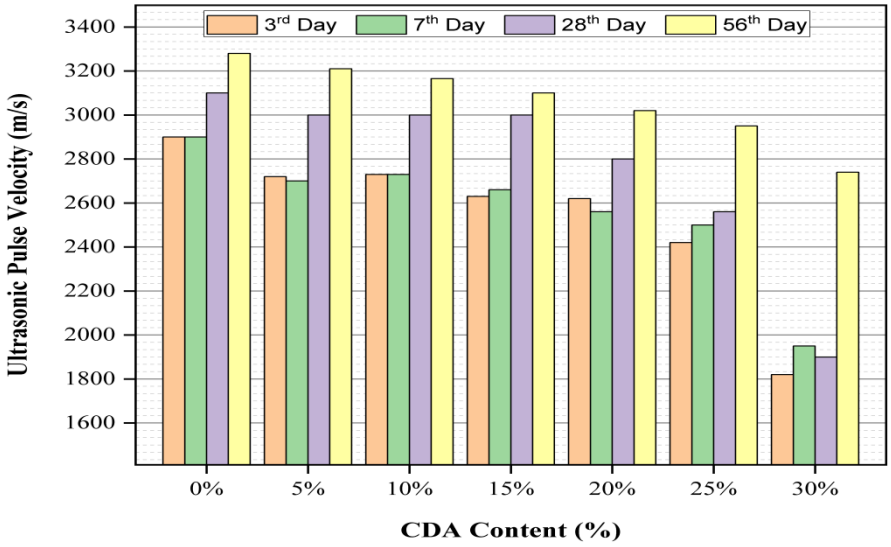

Figure 5. Ultrasonic pulse velocity (UPV) of mortar.

3.2.5. Sulfate Attack Resistance

All of the mortar specimens' ability to withstand sulfate attack was determined by analyzing the variations in their compressive strength following exposure to a sodium sulfate (Na_2SO_4) solution. Figure 6 illustrates the results of the test depicting the variation in compressive strength of mortar containing CDA, subjected to sulfate attack, in comparison to the control mortar sample, at various curing periods. It is evident that the mortar specimens containing up to 10% CDA are able to withstand sulfate attack without much impact on their compressive strength, as the reduction in strength is negligible. Furthermore, it was observed that the compressive strength starts to decrease beyond 15% CDA content, which means that at CDA20 to CDA30, the sodium sulfate significantly affected the strength of the mortar specimens. This phenomenon can be attributed to the high quantity of CaO and the formation of a gel, particularly when the CDA replacement ratio exceeds 10%, as demonstrated by the microstructural tests discussed in Section 3. Consequently, the density of mortar samples decreases, allowing for the diffusion of sulphate ions into the mortar pores. This accelerates the chemical reaction between the hydration products of cement, such as Na_2SO_4 and sulphate ions, with $Ca(OH)_2$ and monosulfate, resulting in the formation of gypsum and ettringite (crystal needles) within the mortar pores [36]. These factors collectively have a negative impact on the mortar's ability to resist sulfate.

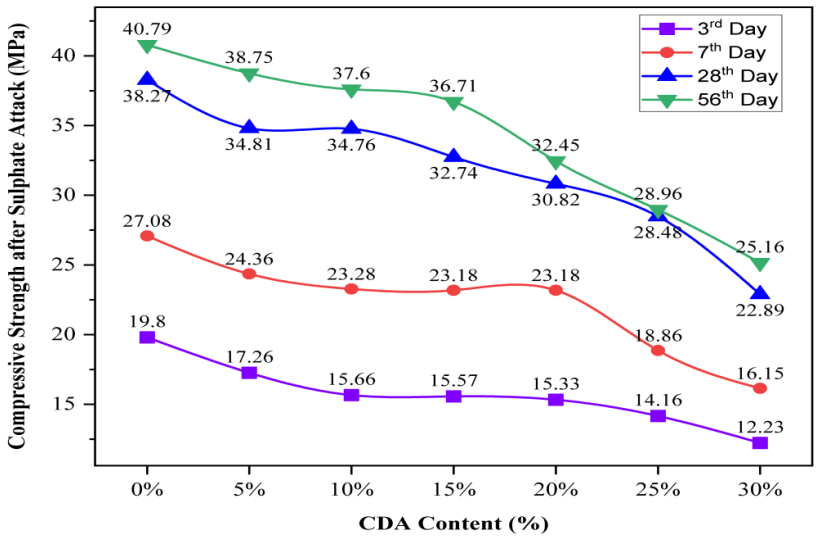

Figure 6. Compressive strength of the mortar specimens after exposure to sulfate attack.

3.3. Effects of CDA on Microstructure of Mortar

3.3.1. Thermal Decomposition

Figures 7–9 illustrate and compare the thermogravimetric (TGA) analyses of mortar samples containing 10%, 20%, and 30% CDA, respectively, after being cured for 28 days. In all figures, the weight loss was determined by subtracting the level of the lower line y-axis from that of the upper line y-axis. According to Figure 7, after 28 days of curing, the mortar sample containing 10% CDA underwent a weight loss of 23% at a heating temperature of 450 °C due to the decomposition of CaO and water from C–H. The weight loss decreased by 8% after an increase in temperature to 500 °C, and then increased again up to a heating temperature of 600 °C. From 600 to 750 °C, the weight loss of the mortar sample significantly decreased by 15% due to the decomposition of water and the C–S–H gel, as well as the carbonation of CO_2 from CO_3. In the case of the 28-day cured mortar sample containing 20% CDA (Figure 8), the trend of thermal stability was almost similar to that of the 10% CDA sample. The mortar samples containing 10% CDA revealed that the $Ca(OH)_2$ dehydrated and lost approximately 25% its weight at a temperature of 450 °C, with only a 7% weight reduction up to 500 °C. Additionally, the figure elucidates that there was no further weight loss when the heating temperature was increased from 500 °C to 550 °C. However, both $CaCO_3$ and the C–S–H gel released CO_2 and water, respectively, and lost 13% of their weight as the temperature increased from 500 °C to 700 °C. Further increases in temperature did not appear to affect the thermal stability of the mortar. The percentage weight loss for the mortar sample containing 30% CDA, which was cured for 28 days, is presented in Figure 9. It can be noticed that the weight loss of the mortar continuously decreased with an increase in temperature up to 450 °C due to the evaporation of water from the C–H gel. It can also be observed that it exhibited a weight loss of 11% due to the evaporation of water from the C–H gel, which was relatively smaller than that of the 10% and 20% CDA mortar samples. Furthermore, the weight loss due to carbonation and dehydroxylation was insignificant compared to the other samples, with a combined weight loss of about 8% at a heating temperature between 450 °C and 700 °C. This indicates that either there were no CaO, CO_2, and H_2O molecules in the C–S–H gel and $CaCO_3$, as all these oxides were released at a temperature of 450 °C, or the heating temperature might not have been sufficient in order to remove the oxides. Generally, for all the mortar samples containing 10%, 20%, and 30% CDA, the thermal stability of 28-day cementitious pastes would not be significantly affected in a temperature range of approximately 500–600 °C.

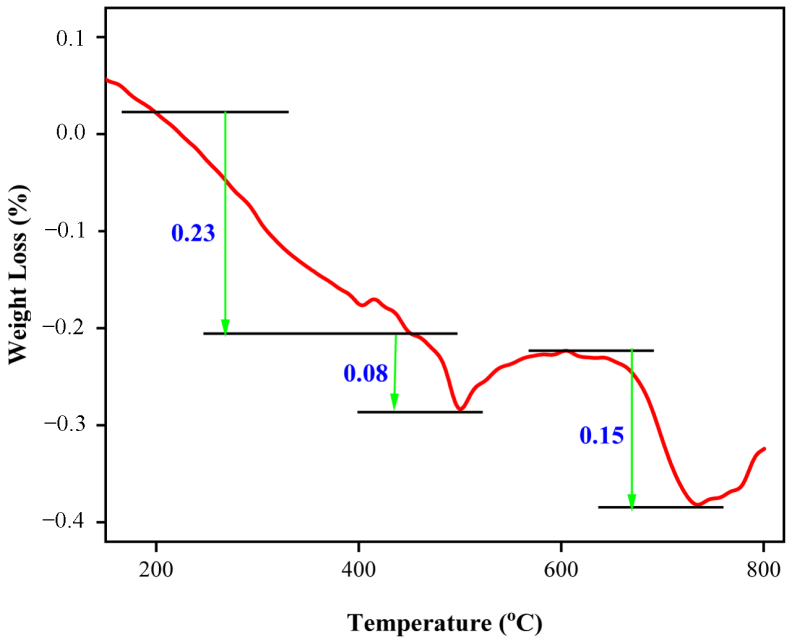

Figure 7. TGA curve of CDA10 after 28 days of curing.

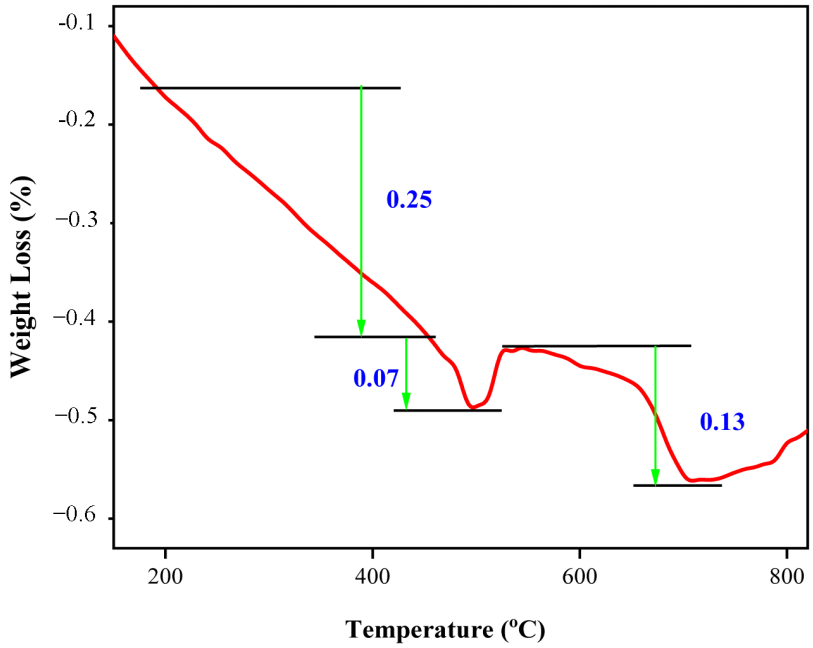

Figure 8. TGA curve of CDA20 after 28 days of curing.

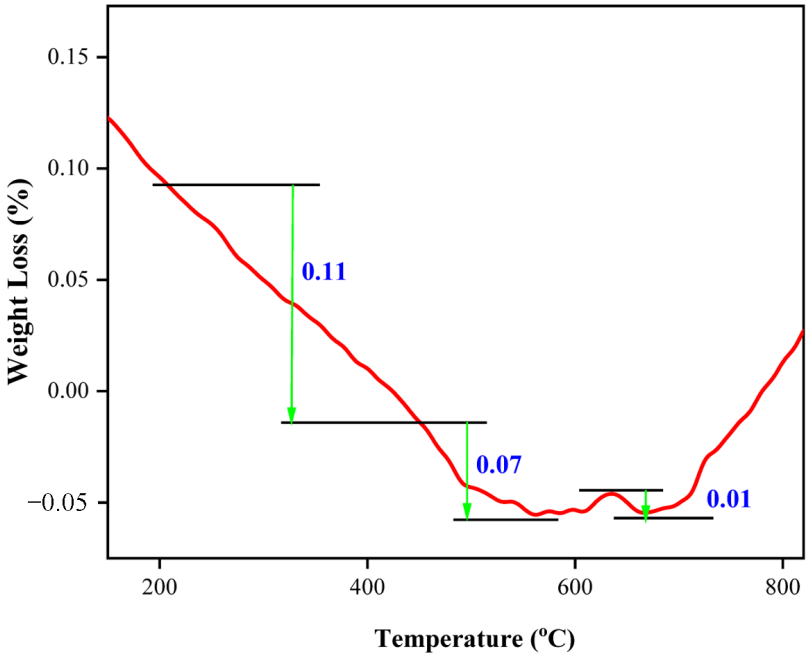

Figure 9. TGA curve of CDA30 after 28 days of curing.

3.3.2. Mineralogical Composition

The result of the Fourier-transform infrared spectroscopy (FTIR) analysis conducted on the mortar samples containing CDA content of 0%, 10%, and 30% after 7 and 28 days of curing is shown in Figures 10 and 11, respectively. The FTIR spectra for the 7-day samples, as shown in Figure 10, reveal major peaks at 3860–3640, 2930–2115, 1750–1345, and 1100–450 cm^{-1}. On the other hand, the spectra for the 28-day samples (Figure 11) exhibit major peaks at 3760–3640, 2930–2280, 2100–1300, 1016–620, and 490–420 cm^{-1}. The wavenumbers, curves, peaks, and valleys observed in the FTIR spectra of the selected mortar samples, i.e., CDA0, CDA10, and CDA30 were almost identical for both curing periods. This suggested that the CDA content had no significant effect on the hydration product during the development of the hydration process, despite minor differences in

wavenumbers observed between the 7th and the 28th day samples. Figure 10 illustrates that unreacted particles were detected at the major peak wavenumbers of 744 cm^{-1} for CDA0 and CDA10 samples. However, for CDA30 samples, the wavenumbers increased and extended to the range of 813–681 cm^{-1}. The abundance of unreacted particles can impede the activation reaction, resulting in a delayed early-age strength development. Additionally, the production of a C–S–H gel was lower in the CDA10 and CDA30 mortars, while CDA0 exhibited superior C–S–H gel production compared to CDA10 and CDA30. The wavenumber band between 1644 and 1000 cm^{-1} indicates the presence of small amounts of carbon and the O–H–O extending and stretching vibration between 3460 and 1727 cm^{-1} suggests the presence of free water.

Based on the FTIR analysis depicted in Figures 10 and 11, the curve pattern observed for 28-day samples were comparable to that of the 7-day samples. Notably, unreacted particles were identified at identical wavenumbers within the range of 780–450 cm^{-1}, with a major peak observed at 700 cm^{-1} for CDA10. The formation of a C–S–H gel was evident from the peak observed at 1016–1115 cm^{-1}. The stretching vibration mode of Si–O–T (T: tetrahedral Si or Al) was assigned to the band observed between 950 and 1200 cm^{-1}. This specific frequency range of 1018–1045 cm^{-1} was noted to be characteristic of the presence of silicon tetrahedra (SiO_4) in the chain structure of the C–S–H gel [37]. Furthermore, both figures provided further insight into the formation of the C–S–H gel, with the frequency range of 1110–970 cm^{-1} indicating its formation. Unreacted particles were observed in the 600–400 cm^{-1} range, while O–H–O was detected in the 3440–2328 cm^{-1} range.

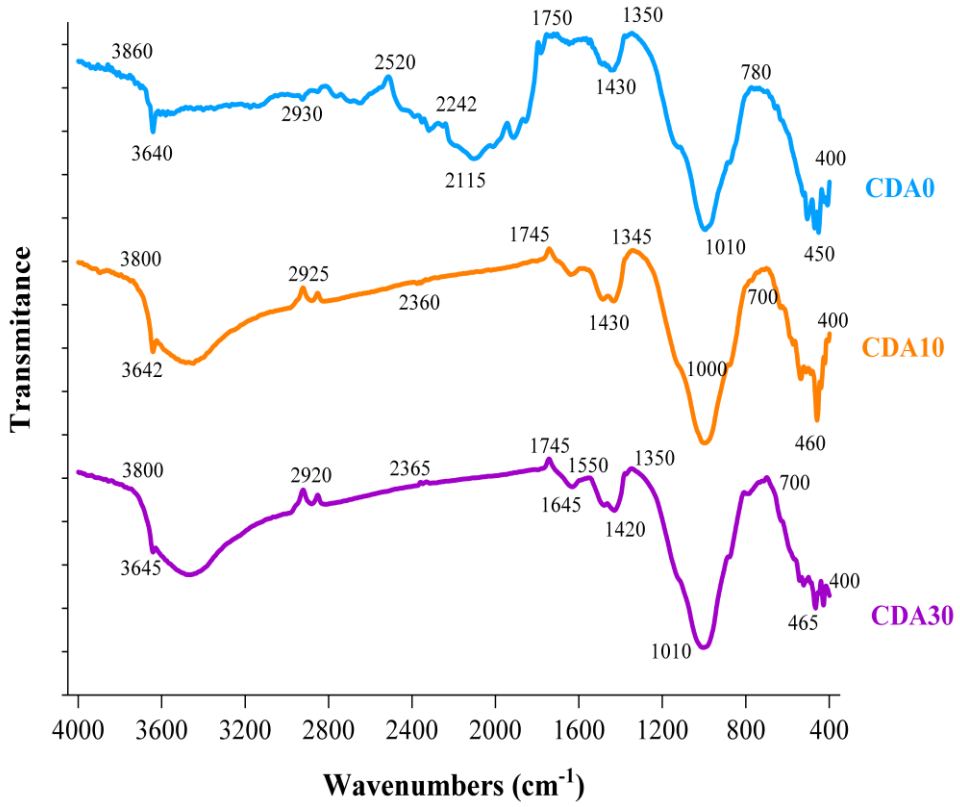

Figure 10. FTIR spectra of paste from a control and CDA-containing mortar cured for seven days.

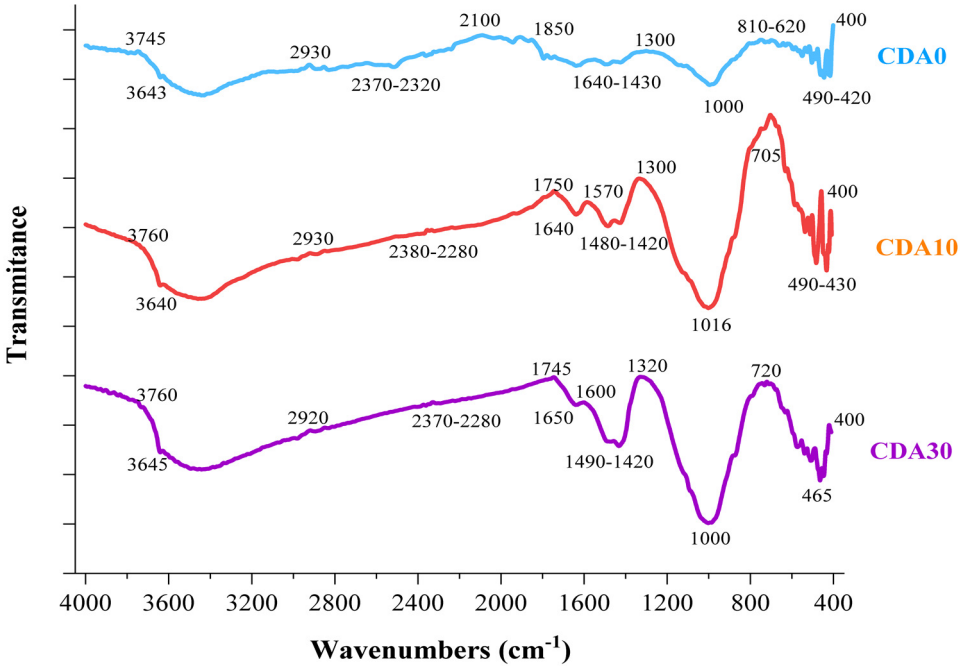

Figure 11. FTIR spectra of paste from a control and CDA-containing mortar cured for 28 days.

4. Conclusions

This research explored the potential use of cow dung ash (CDA) as a supplementary cementitious material by investigating its physical and chemical properties. The study also investigated how CDA in varying proportions (5%, 10%, 15%, 20%, 25%, and 30%) affects the workability, hardened, and microstructural properties of mortar. Based on the results obtained from the study, the following conclusions can be drawn:

- The oxide composition of CDA meets ASTM C150/C150M requirements for cement and is almost similar to that of ordinary Portland cement. However, OPC contains greater amounts of the major oxides of CaO and SiO_2 in comparison to CDA.
- As the percentage of CDA increases in the mortar mix, its workability decreases. Compared to the control mortar, the mortar mixes containing CDA exhibit reduced slump flow. The mortar containing 15% CDA satisfies the slump flow requirements outlined in the ASTM C1437 standard.
- When CDA was utilized beyond 5%, the water absorption of the mortar samples considerably increased due to the porous nature and significant presence of organic compounds that were not effectively removed. As a result, all of the density, homogeneity, and compressive strength of the mortar were negatively impacted. Although the use of CDA as a replacement for OPC resulted in a decrease in compressive strength, the reduction was not considered significant for up to a 15% substitution, as observed at the age of 56 days.
- The compressive strength of mortar specimens is not significantly affected by sulfate attack when containing up to 10% CDA, indicating that these specimens can withstand such an attack with only negligible reduction in strength.
- Mortar mixes containing 10%, 20%, and 30% CDA were found to exhibit thermal stability when exposed to temperatures ranging from 500°C to 600 °C. The FTIR analysis revealed the presence of unreacted particles and a wide-stretched C–S–H gel in the mortar samples.
- While the effect of CDA on the properties of mortar can differ across different tests, replacing OPC with up to 10% CDA can serve as a viable substitute for cementitious materials in mortar production. Adopting CDA as a supplementary cementitious material may offer a sustainable and eco-friendly approach that delivers advantages for both the environment and the construction sector.

- The study has demonstrated the potential of CDA as a promising option for partial replacement of cement. However, further investigations are needed to explore the possible synergistic effects of combining CDA with other supplementary cementitious materials (SCMs), with or without an alkali activator. Such investigations can help to identify the most effective combinations that can lead to improved mechanical properties and durability, as well as sustainable solutions in the cement industry.

Author Contributions: Conceptualization, M.A.W. and M.D.Y.; methodology, M.A.W.; software, M.A.W. and W.Z.T.; validation, M.D.Y., W.Z.T. and B.Z.H.; formal analysis, M.A.W.; investigation, M.A.W.; resources, M.D.Y.; data curation, W.Z.T.; writing—original draft preparation, M.A.W. and B.Z.H.; writing—review and editing, W.Z.T.; visualization, B.Z.H.; supervision, M.D.Y.; project administration, M.D.Y.; funding acquisition, M.D.Y. All authors have read and agreed to the published version of the manuscript.

Funding: This research received no external funding.

Informed Consent Statement: Not applicable.

Data Availability Statement: The data supporting the findings of this study are available upon request.

Conflicts of Interest: The authors declare no conflict of interest.

References

1. Global Cement and Concrete Association (GCCA). *Global Cement and Concrete Industry Announces Roadmap to Achieve Groundbreaking 'Net Zero' CO2 Emissions by 2050*; Global Cement and Concrete Association (GCCA): London, UK, 2021.
2. Lehne, J.; Preston, F. *Making Concrete Change Innovation in Low-Carbon Cement and Concrete*; Policy Commons: London, UK, 2018.
3. Cosentino, I.; Liendo, F.; Arduino, M.; Restuccia, L.; Bensaid, S.; Deorsola, F.; Ferro, G.A. Nano $CaCO_3$ particles in cement mortars towards developing a circular economy in the cement industry. *Procedia Struct. Integr.* **2020**, *26*, 155–165. [CrossRef]
4. Khankhaje, E.; Kim, T.; Jang, H.; Kim, C.-S.; Kim, J.; Rafieizonooz, M. Properties of pervious concrete incorporating fly ash as partial replacement of cement: A review. *Dev. Built Environ.* **2023**, *14*, 100130. [CrossRef]
5. Yehualaw, M.D.; Alemu, M.; Hailemariam, B.Z.; Vo, D.-H.; Taffese, W.Z. Aquatic Weed for Concrete Sustainability. *Sustainability* **2022**, *14*, 15501. [CrossRef]
6. Gedefaw, A.; Worku Yifru, B.; Endale, S.A.; Habtegebreal, B.T.; Yehualaw, M.D. Experimental Investigation on the Effects of Coffee Husk Ash as Partial Replacement of Cement on Concrete Properties. *Adv. Mater. Sci. Eng.* **2022**, *2022*, 4175460. [CrossRef]
7. Duvallet, T.Y.; Jewell, R.B. Recycling of bone ash from animal wastes and by-products in the production of novel cements. *J. Am. Ceram. Soc.* **2023**, *106*, 3720–3735. [CrossRef]
8. Yang, K.H.; Jung, Y.B.; Cho, M.S.; Tae, S.H. Effect of supplementary cementitious materials on reduction of CO_2 emissions from concrete. *J. Clean. Prod.* **2015**, *103*, 774–783. [CrossRef]
9. Endale, S.A.; Taffese, W.Z.; Vo, D.-H.; Yehualaw, M.D. Rice Husk Ash in Concrete. *Sustainability* **2022**, *15*, 137. [CrossRef]
10. Zeybek, Ö.; Özkılıç, Y.O.; Karalar, M.; Çelik, A.İ.; Qaidi, S.; Ahmad, J.; Burduhos-Nergis, D.D.; Burduhos-Nergis, D.P. Influence of Replacing Cement with Waste Glass on Mechanical Properties of Concrete. *Materials* **2022**, *15*, 7513. [CrossRef]
11. Acar, M.C.; Çelik, A.İ.; Kayabaşı, R.; Şener, A.; Özdöner, N.; Özkılıç, Y.O. Production of perlite-based-aerated geopolymer using hydrogen peroxide as eco-friendly material for energy-efficient buildings. *J. Mater. Res. Technol.* **2023**, *24*, 81–99. [CrossRef]
12. Beskopylny, A.N.; Shcherban', E.M.; Stel'makh, S.A.; Meskhi, B.; Shilov, A.A.; Varavka, V.; Evtushenko, A.; Özkılıç, Y.O.; Aksoylu, C.; Karalar, M. Composition Component Influence on Concrete Properties with the Additive of Rubber Tree Seed Shells. *Appl. Sci.* **2022**, *12*, 11744. [CrossRef]
13. Taffese, W.Z. Suitability Investigation of Recycled Concrete Aggregates for Concrete Production: An Experimental Case Study. *Adv. Civ. Eng.* **2018**, *2018*, 8368351. [CrossRef]
14. Basaran, B.; Kalkan, I.; Aksoylu, C.; Özkılıç, Y.O.; Sabri, M.M.S. Effects of Waste Powder, Fine and Coarse Marble Aggregates on Concrete Compressive Strength. *Sustainability* **2022**, *14*, 14388. [CrossRef]
15. Karalar, M.; Bilir, T.; Çavuşlu, M.; Özkiliç, Y.O.; Sabri Sabri, M.M. Use of recycled coal bottom ash in reinforced concrete beams as replacement for aggregate. *Front. Mater.* **2022**, *9*, 1064604. [CrossRef]
16. Shcherban', E.M.; Stel'makh, S.A.; Beskopylny, A.N.; Mailyan, L.R.; Meskhi, B.; Shilov, A.A.; Chernil'nik, A.; Özkılıç, Y.O.; Aksoylu, C. Normal-Weight Concrete with Improved Stress–Strain Characteristics Reinforced with Dispersed Coconut Fibers. *Appl. Sci.* **2022**, *12*, 11734. [CrossRef]
17. Çelik, A.İ.; Özkılıç, Y.O.; Zeybek, Ö.; Karalar, M.; Qaidi, S.; Ahmad, J.; Burduhos-Nergis, D.D.; Bejinariu, C. Mechanical Behavior of Crushed Waste Glass as Replacement of Aggregates. *Materials* **2022**, *15*, 8093. [CrossRef]
18. Karalar, M.; Özkılıç, Y.O.; Aksoylu, C.; Sabri, M.M.S. Flexural behavior of reinforced concrete beams using waste marble powder towards application of sustainable concrete. *Front. Mater.* **2022**, *9*, 1068791. [CrossRef]

19. Ige, J.A.; Olojo, F.O. Effect of Cow Dung Ash Calcined at Different Temperature on the Geotechnical Properties of Laterite Soil. *J. Archit. Civ. Eng.* **2021**, *6*, 38–47.
20. Ojedokun, O. Cow Dung Ash (CDA) as Partial Replacement of Cementing Material in the Production of Concrete. *Br. J. Appl. Sci. Technol.* **2014**, *4*, 3445–3454. [CrossRef]
21. Ekasila, S.; Vishali, B.; Anisuddin, S. An experimental investigation on compressive strength of concrete with rice husk and cow dunk ash using various curing methods. *Mater. Today Proc.* **2022**, *52*, 1182–1188. [CrossRef]
22. Ramachandran, D.; Vishwakarma, V.; Viswanathan, K. Detailed studies of cow dung ash modified concrete exposed in fresh water. *J. Build. Eng.* **2018**, *20*, 173–178. [CrossRef]
23. Pappis, I.; Sahlberg, A.; Walle, T.; Broad, O.; Eludoyin, E.; Howells, M.; Usher, W. Influence of Electrification Pathways in the Electricity Sector of Ethiopia—Policy Implications Linking Spatial Electrification Analysis and Medium to Long-Term Energy Planning. *Energies* **2021**, *14*, 1209. [CrossRef]
24. Taffese, W.Z.; Abegaz, K.A. Embodied Energy and CO_2 Emissions of Widely Used Building Materials: The Ethiopian Context. *Buildings* **2019**, *9*, 136. [CrossRef]
25. *ASTM C1084-19*; Standard Test Method for Portland-Cement Content of Hardened Hydraulic-Cement Concrete. ASTM International: West Conshohocken, PA, USA, 2020.
26. *ASTM C150/C150M-22*; Standard Specification for Portland Cement. ASTM International: West Conshohocken, PA, USA, 2022.
27. *ASTM C117-17*; Standard Test Method for Materials Finer than 75-µm (No. 200) Sieve in Mineral Aggregates by Washing. ASTM International: West Conshohocken, PA, USA, 2020.
28. Zhou, S.; Zhang, S.; Shen, J.; Guo, W. Effect of cattle manure ash's particle size on compression strength of concrete. *Case Stud. Constr. Mater.* **2019**, *10*, e00215. [CrossRef]
29. Venkatasubramanian, C.; Muthu, D.; Aswini, G.; Nandhini, G.; Muhilini, K. Experimental studies on effect of cow dung ash (pozzolanic binder) and coconut fiber on strength properties of concrete. *IOP Conf. Ser. Earth Environ. Sci.* **2017**, *80*, 012012. [CrossRef]
30. Sruthy, B.; Mathew, G.M.; Krishnan, A.G.; Raj, S.G. An Experimental Investigation on Strength of Concrete Made with Cow Dung Ash and Glass Fibre. *Int. J. Eng. Res.* **2017**, *6*, 492–495. [CrossRef]
31. Rawal, H.M.; Deshmukh, M.; Patil, J. Partial Replacement of Cow Dung with Cement. *Int. J. Sci. Res. Eng. Trends* **2019**, *5*, 518–521.
32. *ASTM C1585-20*; Standard Test Method for Measurement of Rate of Absorption of Water by Hydraulic-Cement Concretes. ASTM International: West Conshohocken, PA, USA, 2020.
33. Azhar, N.S.D.M.; Zainal, F.F.; Abdullah, M.M.A.B. *Effect of Geopolymer Paste on Compressive Strength, Water Absorption and Porosity*; AIP Publishing LLC: Melville, NY, USA, 2020. [CrossRef]
34. *IS 2250*; Code of Practice for Preparation and Use of Masonry Mortars. Bureau of Indian Standards: Delhi, India, 1981.
35. *IS 13311 (Part 1)*; Method of Non-Destructive Testing of Concrete, Part 1: Ultrasonic Pulse Velocity. Bureau of Indian Standards: Delhi, India, 1992.
36. Nawaz, M.A.; Ali, B.; Qureshi, L.A.; Aslam HM, U.; Hussain, I.; Masood, B.; Raza, S.S. Effect of sulfate activator on mechanical and durability properties of concrete incorporating low calcium fly ash. *Case Stud. Constr. Mater.* **2020**, *13*, e00407. [CrossRef]
37. Hwang, C.L.; Yehualaw, M.D.; Vo, D.H.; Huynh, T.; Largo, A. Performance evaluation of alkali activated mortar containing high volume of waste brick powder blended with ground granulated blast furnace slag cured at ambient temperature. *Constr. Build. Mater.* **2019**, *223*, 657–667. [CrossRef]

Disclaimer/Publisher's Note: The statements, opinions and data contained in all publications are solely those of the individual author(s) and contributor(s) and not of MDPI and/or the editor(s). MDPI and/or the editor(s) disclaim responsibility for any injury to people or property resulting from any ideas, methods, instructions or products referred to in the content.